AAC Accepts, published online ahead of print on 4 October 2010
Antimicrob. Agents Chemother. doi:10.1128/AAC.01050-10

Mechanism of Antifungal Activity of Terpenoid Phenols Resembles Calcium Stress and Inhibition of the TOR Pathway

Anjana Rao*[1], Yongqiang Zhang*[2], Sabina Muend*[3] and Rajini Rao[2#]

From the Department of Physiology, Johns Hopkins University School of Medicine

Running Title: Antifungal Mechanism of Carvacrol

*these authors contributed equally to this work

[1]current address: Smith College, 1 Chapin Way, Northampton, MA

[3]current address: Naval Survival Training Institute, 55 Radford Blvd., Pensacola, FL

[#]To whom correspondence should be addressed: Department of Physiology, Johns Hopkins University School of Medicine, 725 N. Wolfe Street, Baltimore MD 21205. Phone: 410 955 4732; Email: rrao@jhmi.edu

ABSTRACT

Terpenoid phenols, including carvacrol, are components of plant essential oils that exhibit potent antifungal activity against a wide range of pathogens, including *Candida albicans*, *Staphylococcus aureus* and *Pseudomonas aeruginosa*. To gain a mechanistic view of the cellular response to terpenoid phenols, we used *Saccharomyces cerevisiae* as a model organism and monitored temporal changes in metabolic activity, cytosolic and vacuolar pH and Ca^{2+} transients. Using a panel of related compounds, we observed dose dependent Ca^{2+} bursts that correlated with antifungal efficacy. Changes in pH were long lasting and followed the Ca^{2+} transients. A *vma* mutant lacking functional V-ATPase and defective in ion homeostasis was hypersensitive to carvacrol toxicity, consistent with a role for ionic disruptions in mediating cell death. Genomic profiling within 15 min. of exposure revealed a robust transcriptional response to carvacrol, closely resembling that of calcium stress. Genes involved in alternate metabolic and energy pathways, stress response, autophagy and drug efflux were prominently up regulated whereas repressed genes mediated ribosome biogenesis and RNA metabolism. These responses were strongly reminiscent of the effects of rapamycin, the inhibitor of TOR pathway of nutrient sensing. The results point to the activation of specific signaling pathways downstream of cellular interaction with carvacrol, rather than a non-specific lesion of membranes as has been previously proposed.

INTRODUCTION

While the medicinal properties of herbs have been recognized since ancient times, there has been a resurgence of interest in the antimicrobial properties of botanical extracts. Essential oils have been amply documented to kill a wide range of pathogenic fungi and bacteria such as *Candida albicans, Staphylococcus aureus* and *Pseudomonas aeruginosa,* including their drug resistant variants (*6*, *22*, *10*, *21*). Of the herbal extracts tested, essential oils derived from the genus *Oreganum* were among the most effective, with *in-vitro* MIC of 500 ppm against *C. albicans* (*26*). Major components of Oregano extract, which include the terpenoid phenols carvacrol, thymol and eugenol, have potent antifungal activity on their own (*23*, *24*, *4*). Terpenoid phenols have been shown to be efficacious not only on planktonic cells, but also on biofilms of *Candida albicans* that are resistant to many antifungal drugs. Carvacrol demonstrated the strongest antifungal activity against *Candida albicans* biofilms with a MIC of <0.03% (*9*). Furthermore, carvacrol was shown to be effective regardless of the maturity of the biofilm. The terpenoid phenols tested were able to inhibit biofilms of not only *Candida albicans*, but five other strains of this pathogen, as well as *C. glabrata* and *C. parapsilosis*. In addition to their antimycotic, antibacterial, insecticidal and bioherbicidal properties, essential oils are also well known for their anti-oxidant characteristics and are used to inhibit lipid peroxidation in preventing food spoilage or as chemoprotective agents in the treatment of various diseases including cancer (*26*, *1*).

Although there is abundant evidence for antifungal efficacy of essential oils and their constituents, there has been relatively little work on the mechanism of killing. A better understanding of the cellular basis of these antifungal agents would improve their

1 therapeutic potential by guiding combination therapy with other established drugs and
2 lead to safer and more innovative treatments. Baker's yeast offers a sophisticated toolkit
3 of experimental approaches. We establish *Saccharomyces cerevisiae* as a model organism
4 for exploring the effect of terpenoid phenols at a cellular and molecular level. We used
5 compartment-specific cellular probes to follow temporal changes in metabolic activity,
6 Ca^{2+} and pH as a function of toxicity. Genome-wide profiling of the transcriptional
7 changes to carvacrol revealed large and rapid metabolic, biosynthetic and stress responses
8 that provide molecular insight into the mechanism of action of essential oils.

MATERIALS AND METHODS

Essential Oils and Phenolic compounds: Medicinal grade oregano oil was purchased from a local health store. Carvacrol, thymol, eugenol, vanillin, guaicol, *p*-cymene and γ-terpinene were purchased from Sigma-Aldrich and were at 98% purity. Carvacrol was in liquid form (density, 0.976 g/cm^3). Thymol, a white powder, was made into a 10% stock solution in ethanol. Each compound was made into 10%, 1% and 0.1% stocks by serial dilutions in ethanol and stored at room temperature.

Yeast Toxicity Assays: BY4742 (*MATα his3Δ1 leu2Δ0 lys2Δ0 ura3Δ0*) was grown overnight in a shaking incubator in SC medium as specified by Sherman (*25*). Absorbance was measured at 600 nm after 1:10 dilution in water. Cells (0.025 O.D.) were added to 1 ml SC medium in each well of a 24 well plate. Finally, the phenolic compounds to be tested were added, in triplicate, to the specified final concentrations. The plates were stored overnight in a 30ºC incubator. The plates were gently vortexed to resuspend cells before measurement of Absorbance at 600 nm. Halo formation was assessed after soaking sterile filter paper in dilutions of essential oil and overlaying a lawn of freshly plated *S. cerevisiae* on SC medium. Plates were incubated at 30ºC for 1-2 days. Mineral oil was used for dilution and as control.

FUN-1 fluorescence: The fluorescence indicator FUN-1 (Invitrogen) was used to monitor the loss of metabolic activity according to Millard *et al.* (*19*), as previously described (*20*). Cells emitting green fluorescence were considered metabolically inactive (*19*). To load the cells with dye, the optical density (OD at 600 nm) of the yeast culture was measured, and the cells were collected by centrifugation, and resuspended in 100 µl

of SC media and 2 µl of FUN-1 dye. The tubes were vortexed, wrapped in foil, and then incubated at 30˚C for an hour. Cells were washed twice with 2% glucose and cell pellet resuspended in 2 ml per OD. To 50 µl of cells, 5 µl of mineral oil or Oregano oil was added. After 15 minutes, the cells were observed under a fluorescence microscope. To quantify these results, 5, 10, and 25 µl of each compound was added, in triplicate, to the cells in a black 96-well microtiter well plate. The final volume was 200 µl. Fluorescence (emission 575 nm) was measured for two hours in a using a BMG Fluostar Optima plate reader. Averages of the triplicates were graphed against time.

Ca^{2+}-dependent aequorin luminescence: BY4742 transformed with plasmid pEVP11-Aeq-89 expressing aequorin was grown overnight in SC medium (*20*). One unit of OD_{600} of cells was spun down per microfuge tube. The cell pellets were resuspended in 1 ml of 2% Glucose and spun and decanted again. 50 µl of SC was added into each tube. After vortexing to mix cells, 6 µl of coelenterazine (Invitrogen; 12.5 mg/ml in ethanol, stored at -20˚C) was added into each tube. The cells were incubated for two hours in a 30˚C incubator to allow reconstitution of aequorin with coelenterazine. Finally, cells were spun down and transferred into 2 ml of SC. After vortexing again, 150 µl was placed in each well of a white 96 well microtiter plate. In addition to this, 150 µl of cells was also put into another microtiter plate to read OD. The drug was added (0.0125, 0.25, 0.5 and 0.1 %) in accordance to the figure legend and luminescence measured on a Fluostar Optima microplate reader. Each dose of drug was done in duplicate and the experiment was repeated at least two times. Luminescence values were collected every second, normalized to the OD and averaged.

pH Measurements: Cytoplasmic pH was measured using pHluorin, essentially as described (*8*). Briefly, BY4742 was transformed with plasmid pZR4.1 (*33*), grown to mid-logarithmic phase and transferred to clear bottom 96-well black plates. Carvacrol was injected at the indicated concentration and fluorescence (dual excitation at 410 and 485 nm and emission at 520 nm) was recorded in a BMG Fluostar Optima plate reader. Calibrations were done in buffers of known pH as described (*8*). Vacuolar pH was measured after loading with BCECF AM (Invitrogen), a pH sensitive fluorophore that localizes preferentially in the vacuole (*3*). Cells were loaded with BCECF AM and transferred to a 96-well plate. Fluorescence (dual excitation at 450 and 485 nm and emission at 520 nm) was measured in response to carvacrol and calibrated as previously described (*3*).

DNA microarray: Early log phase culture of *S. cerevisiae* BY4742 (OD 0.1) was treated with carvacrol at 0.005% and 0.01% for 15 minutes. RNA was isolated from control and carvacrol treated cells as described previously (*32*). Integrity of the RNA samples was confirmed by polyacrylamide gel electrophoresis. cDNA synthesis, labeling and hybridization, image scanning and processing were conducted at the Johns Hopkins Microarray Core Facility as described previously. Microarray data were imported to Partek GS software for normalization and analysis. The data set was then imported to Gene Cluster 3.0 for hierarchical clustering analyses, along with previously published DNA microarray data for these genes in response to thymol (*7*), $CaCl_2$, (*31*), rapamycin (*16*), amiodarone (*32*), nitrogen depletion and growth in YPD (*14*), diauxic shift (*11*), and four classes of antifungals (caspofungin, ketoconazole, 5-fluorocytosine, amphotericin; *2*), downloaded from publisher's website or requested from the authors. Results were

displayed with Java Tree View software and edited in Adobe Photoshop (Adobe Systems Inc.). Geneset enrichment analyses were performed on the server at Munich Information center for Protein Sequences (MIPS) database (http://mips.gsf.de/proj/funcatDB/search_main_frame.html).

RESULTS AND DISCUSSION

Efficacy of Oregano oils and phenolic derivatives against *S. cerevisiae*

A first step in our study was to determine whether the susceptibility of *S. cerevisiae* to terpenoid phenols recapitulated published studies in various pathogenic fungi. The strength of Oregano Oil was analyzed by looking at the dose dependence of halo formation on a lawn of yeast. Oregano Oil effectively prevented yeast growth up to a dilution of 1:8 (Fig. 1A) and no colonies appeared even after prolonged incubation consistent with potent fungicidal activity. By comparison, another essential oil with antifungal activity, Tea Tree (or Melaleuca) Oil only worked well at full strength and small colonies appeared around the filters after two weeks (data not shown), suggesting a more fungistatic mechanism of action. As control, we showed that mineral oil had no effect on yeast growth. In metabolically active cells, the vital stain FUN-1 is converted to a red intravacuolar spindle-like structure, whereas loss of metabolic activity is associated with bright greenish yellow fluorescence (*19*). In yeast cells treated briefly (15 min) with Oregano oil, but not mineral oil, FUN-1 green fluorescence was indicative of a loss of metabolic activity (Fig. 1B).

Next, we evaluated the relative efficacy of purified components of oregano oil and related compounds. The monoterpenoid phenol carvacrol, and its structural isomer thymol together constitute 72-83% of extracts from *Origanum vulgarum* species, although they vary reciprocally as predominant components in distinct chemotypes (*23*). Out of a panel of structurally related phenolic compounds (Fig. 1C lower panel), carvacrol was found to be most potent in inhibiting yeast growth, with MIC of 0.008%

(or 79.8 μg/ml), which was 1,500 times more effective than Oregano oil (Fig. 1A). Thymol was only slightly less efficacious whereas eugenol, a major phenolic component of clove oil (*Eugenia* sp.), was significantly less effective in the yeast growth assay relative to carvacrol (Fig. 1C). In contrast, the monoterpene hydrocarbon γ-terpinene, which is the biosynthetic precursor of carvacrol and also a component of Oregano oil, was ineffective as a fungicide in the same concentration range as the terpenoid phenols. Other phenolic compounds, vanillin and guaiacol, were also ineffective as fungicides (Fig. 1C). These results parallel the work of Tampieri *et al*. (*27*), showing that out of a panel of terpenoid phenols, carvacrol was the most effective in killing *C. albicans* at a MIC of 100 ppm. Eugenol was slightly less active (MIC=250 ppm) than carvacrol, and methyl eugenol was even weaker (MIC=1000 ppm). Unlike carvacrol, which has a free hydroxyl group, eugenol has a methylated hydroxyl group, and methyl eugenol has two methyl groups. Similarly, hydroxymethyl derivatives of carvacrol, thymol and eugenol had significantly lower antifungal activity relative to the parent compounds (*18*), although interestingly, the derivatives had superior free radical scavenging activity and protective effects as antioxidants. This suggests that antifungal activity depends on the structure and make up of the terpenoid phenols, specifically the presence of a free hydroxyl group and an aromatic ring.

Carvacrol exerted dose dependent inhibition on yeast growth rate, with complete inhibition of growth at 0.01%, as shown in Fig. 1D. Quantification of FUN-1 fluorescence showed that carvacrol elicited dose-dependent loss of metabolic activity in yeast (Fig. 1E), more potent than the parent essential oil mixture (not shown), confirming that it was the major active ingredient of Oregano oil.

Carvacrol disrupts ion homeostasis in yeast

We have previously shown that an unrelated membrane active compound, amiodarone, elicits cytosolic Ca^{2+} bursts in yeast, and downstream Ca^{2+} related stress responses (*15, 20, 33*). Therefore, we examined the effect of carvacrol on cytosolic Ca^{2+} levels in yeast expressing the protein aequorin, after reconstitution with its cofactor coelenterazine. The aequorin-coelenterazine complex emits light upon binding to Ca^{2+} and luminescence intensity quantitatively correlates to Ca^{2+} concentration. Upon addition of carvacrol to final concentrations ranging from 0.0125-0.05%, we observed immediate dose-dependent Ca^{2+} elevations, followed by a decrease to baseline within 1-2 minutes (Fig. 2A). These characteristic spikes have been described before (*15, 20, 33*) are consistent with rapid influx of Ca^{2+} from the extracellular medium and from the vacuole and other intracellular stores, followed by sequestration into stores or efflux from cells, and concomitant desensitization of channels. Similar Ca^{2+} bursts were observed with the structural isomer thymol, whereas eugenol showed smaller amplitudes of burst and the remaining compounds tested (vanillin, guaiacol, γ-terpinene and *p*-cymene) failed to elicit any luminescence change (Fig. 2B). Overall, the ability of phenolic compounds to elicit Ca^{2+} bursts correlated well with their antifungal activity (Fig. 1C).

Cytosolic Ca^{2+} levels are tightly controlled within a narrow range compatible with cellular viability by an array of ion pumps and transporters. To distinguish whether the Ca^{2+} burst was directly in the pathway leading to cell death or a mere bystander effect, we evaluated carvacrol toxicity in a yeast *vma2Δ* mutant lacking a functional vacuolar H^+

pump. In the absence of vacuolar acidification, which provides the driving force for H^+-coupled Ca^{2+} exchangers, clearance of cytosolic Ca^{2+} is severely impaired (*12*, *15, 33*). We show that *vma2Δ* mutants are clearly more sensitive to growth inhibition by carvacrol relative to the isogenic wild type, consistent with toxicity of the Ca^{2+} burst (Fig. 2C).

Since the vacuolar H^+ pump is also critical for pH homeostasis (*17*), we monitored the effect of carvacrol on both vacuolar and cytosolic pH. Cells were loaded with the acetoxymethyl derivative of the pH sensitive fluorescent dye, BCECF, which has been shown to stably accumulate in yeast vacuoles (*3*). Addition of carvacrol elicited a 0.5 unit increase in the vacuolar pH and persistent alkalinization (Fig. 2D), suggesting a loss of protons out of the vacuolar lumen. Concurrently, carvacrol was able to induce immediate acidification of the yeast cytosol (Fig. 2E), which was monitored by the pH-dependent fluorescence of the GFP-derivative, pHluorin (*8*). Acidification was dose dependent: whereas 0.01% carvacrol elicited a modest drop in pH, 0.05% carvacrol resulted in an immediate drop in pH of ~0.5 pH unit, followed by a precipitous decrease beginning around 30 min. after exposure to the phenolic compound. This second phase of cytosolic acidification induced by 0.05% carvacrol correlated with a reciprocal increase in vacuolar pH (Fig. 2D) and was well downstream of the Ca^{2+} burst (Fig. 2A). We conclude that carvacrol disrupts both Ca^{2+} and H^+ homeostasis in yeast and that these disruptions likely lead to loss of cell viability.

Transcriptional profiling in carvacrol resembles Ca^{2+} stress response

As an independent approach towards elucidating the antifungal mechanism of terpenoid phenols, we analyzed the transcriptional response to carvacrol in yeast.

Because disruption of Ca^{2+} and H^{+} homeostasis and loss of metabolic activity occur within minutes of carvacrol treatment, we reasoned that 15 minutes following drug exposure would be the ideal time to capture the transcriptional effect of carvacrol. Exponentially growing cells were treated for 15 min with 0.005% and 0.01% carvacrol. These concentrations were shown to cause about half maximal and maximal inhibition of growth rates, relative to control (Fig. 1D).

As summarized in Table 1, the number of gene transcripts showing 2-fold or greater up-regulation increased from 492 to 800 in 0.005% and 0.01% carvacrol respectively, with 91 genes showing robust (≥2-fold) dose-dependent increase at higher carvacrol concentrations. A fewer number of gene transcripts were down-regulated in carvacrol (Table 1).

The functional categories of genes, according to the MIPS classification, that were differentially regulated by at least 2-fold in response to 0.01% carvacrol are shown in Fig. 3. The inner circle depicts the functional distribution of the yeast proteome, whereas the outer circle represents categories that were significantly overrepresented in the carvacrol data sets (*P* values $\leq 5 \times 10^{-3}$). Prominent among up-regulated genes (Fig. 3A) were functions associated with alternative metabolic or energy handling pathways, including glucogen and trehalose biosynthesis, polyamine degradation and fatty acid transport and oxidation. Next in abundance were pathways associated with stress response/signaling and cell rescue, including sporulation, oxygen and free radical detoxificaton, heat shock proteins and chaperones, autophagy and vacuolar degradation mechanisms (Fig. 3A and Table 2). A robust induction of drug efflux mechanisms was observed, including many

members of the ABC drug transporter family such as SNQ2, YOR1, PDR5, PDR10 and PDR15 (Table 2). In contrast to this broad array of cellular functions impacted by carvacrol, pathways represented by repressed (Fig. 3B) genes were overwhelmingly associated with nucleic acid metabolism, RNA synthesis, processing and modification. In dividing cells most of the gene transcription (>80% of nucleotides used) is dedicated to synthesis of ribosomes and tRNA (*28*). Carvacrol rapidly shut down these pathways, consistent with cessation of growth (Table 2; Fig. 1D).

Transcriptional profiles have been documented in response to a wide array of antifungal drugs (5-fluorocytosine, amphotericin B, caspofungin and ketoconozole), metabolic conditions (diauxic shift, nitrogen depletion, rapamycin treatment, YPD) and agents known to induce ionic stress (amiodarone, Ca^{2+}). Clustering analysis of microarray data revealed that the transcriptional response to carvacrol most closely resembled Ca^{2+} stress response (Fig. 4A). We had previously observed that transcriptional response to the antifungal agent amiodarone also clusters closely with Ca^{2+} stress, consistent with the ability of amiodarone to evoke bursts of cellular Ca^{2+}. Here we show a similarity in overall gene regulation by carvacrol and amiodarone (Fig. 4A). These observations corroborate our hypothesis that carvacrol elicits Ca^{2+} mediated cell death. Interestingly, the carvacrol response also closely resembles the effect of rapamycin, an inhibitor of the TOR signaling pathway that controls cell growth in response to nutrients and stress by regulating mRNA transcription and stability, protein translation, ribosome biogenesis and autophagy, and nutrient transport. To examine this further, we evaluated the overlap in transcriptional profile in response to carvacrol, rapamycin and Ca^{2+} stress (Fig. 4 B and C). As seen in the Venn depictions, the overall

transcriptional response to carvacrol was 58% identical to rapamycin and 63% to Ca^{2+} stress. Of the genes up-regulated by carvacrol, a third (166) were also induced by the other two conditions and chiefly included genes involved in metabolic pathways of carbohydrate, protein or energy. An even greater overlap existed among down regulated genes, wherein 60% of genes repressed by carvacrol (257) were common to Ca^{2+} stress and rapamycin. Shared genes belonged largely to categories of RNA metabolism (60.7%) or ribosome biogenesis (55.6%). As these transcriptional responses are characteristic of inhibition of TOR pathway, these findings raise the intriguing possibility that carvacrol may impact the TOR pathway, either independently or through calcium signaling. A recent screen of >3,500 compounds identified amiodarone as an inhibitor of mTORC1, based on the induction of autophagy in nutrient rich medium (*5*); a similar effect may be predicted with carvacrol, given the robust induction of autophagy genes observed (Table 2).

Recently, Bi et al. (*7*) described the transcriptional response of *S. cerevisiae* to thymol, the structural isomer of carvacrol. As shown by hierarchical clustering analysis (Fig. 4A), transcriptional responses to carvacrol and thymol were similar. As both compounds induce rapid and robust cytosolic calcium surge (Fig. 1 A and B), the mechanisms by which these two phenolic isomers kill fungal cells are likely to be substantially similar. We also noted differences in the transcriptional response to the two isomers. Thymol repressed multiple genes implicated in thiamine (vitamin B1) biosynthesis (*THI4, THI6, THI12, THI20, THI21, SNZ2, SNZ3, PET18*) and sulfur metabolism, while this response was not observed after carvacrol treatment. It is possible that these differences represent distinct cellular responses to the two isomers. However,

given the difference in the time of assessment of transcriptional responses to thymol (90 minutes; *7*) and carvacrol (15 minutes, this study), it may well be that induction of sulfur metabolism and repression of thiamine biosynthesis are both late-stage transcriptional responses to these compounds. Furthermore, the size of the transcriptional response appears to substantially diminish with time, with differential regulation of 922 genes by at least two-fold after 15 min exposure to carvacrol (0.005%; see Table 1) and 305 genes after 90 min treatment with thymol (*7*), at equivalent drug concentrations. A similar transient transcriptional response has been previously observed for the membrane-active drug amiodarone, which also elicits a rapid transcriptional response peaking between 10-15 min, followed by significant decay at 30 min (*13*). Thus, we speculate that the study of Bi et al. provides insight into a later window of cellular response that is distinct from the early observations described in this work.

Mechanism of action of terpenoid phenols

The hydrophobic nature of terpenoid phenols ensures their preferential partition into the lipid membrane: thus, carvacrol has log *P* value of 3.26 for partition into phosphatidylethanolamine membranes relative to buffer (*28*). However, hydrophobicity alone does not ensure toxicity since *p*-cymene, a precursor of carvacrol, has higher partition coefficient for lipid membranes but is non-toxic. The presence of the hydroxyl group is critical for toxicity, as seen by lack of microbicidal effects of *p*-cymene and carvacrol methylesters (*28*, *6*). It has been proposed that the delocalized electron system in carvacrol facilitates the dissociation of H^+ from the –OH group. This, in turn, would allow carvacrol to shuttle H^+ and monovalent cations such as K^+ across membranes, dissipating pH and K^+ gradients across cell membranes (*28*). Consistent with this

mechanism, carvacrol was also shown to depolarize bacterial cell membranes and decrease accumulation of the fluorescent dye 5(6)-carboxyfluorescein diacetate, suggestive of an increase in membrane permeability (*30*). Such a mechanism, however, does not explain the transient Ca^{2+} bursts associated with cellular interaction with carvacrol. It may be that effects on membrane expansion and fluidity (*28*) cause opening of ion channels followed by their rapid desensitization.

The distinct phases of Ca^{2+} and pH transients argue against a simple mechanism involving catastrophic membrane lesion, based on the uptake of propidium iodide, as has been previously proposed (*24*, *21*). Propidium iodide staining of cells at MIC confirms cell death, but does not elucidate the mechanisms leading up to cell death and loss of membrane integrity. The transient nature of cytosolic Ca^{2+} surge upon exposure to carvacrol indicates that cells maintain their ability to regulate ion flux (Fig. 2A). In addition, the robust transcriptional responses that largely overlap Ca^{2+} stress and nutrient starvation point to the activation of specific signaling pathways downstream of membrane interaction with terpenoid phenols. These signaling cascades reveal additional fungal targets that can be used in combination with carvacrol and similar essential oil components. Recent studies have shown that azole drugs inhibit vacuolar acidification and exacerbate Ca^{2+} transients elicited by amiodarone, consistent with synergic effects of these drugs (*33*). Future studies could examine potential interactions between essential oils and azoles. In addition, calcineurin inhibitors (cyclosporine A, FK506) that enhance Ca^{2+} dysregulation, and rapamycin analogs that block TOR signaling, could be tested for drug interactions with carvacrol against pathogenic fungi.

Acknowledgments: This work was supported by a grant from the National Institutes of Health, NIAID R01AI065983 to R.R.

References

1. Abdel-Massih, R.M., Fares, R., Bazzi, S., El-Chami, N., Baydoun, E. 2010. The apoptotic and anti-proliferative activity of Origanum majorana extracts on human leukemic cell line. *Leuk Res*. 34:1052-6.

2. Agarwal, A. K., Rogers, P. D., Baerson, S. R., Jacob, M. R., Barker, K. S., Cleary, J. D., Walker, L. A., Nagle, D. G., and Clark, A. M. 2003. Genome wide expression profiling of the response to polyene, pyrimidine, azole, and echinocandin antifungal agents. *J. Biol. Chem*. 278: 34998-35015.

3. Ali, R., Brett, C.L., Mukherjee, S., Rao, R. 2004. Inhibition of sodium/proton exchange by a Rab-GTPase-activating protein regulates endosomal traffic in yeast. *J Biol Chem*. 279:4498-506.

4. Alma, M.H., Mavi, A., Yildirim, A., Digrak, M., Hirata, T. 2003. Screening chemical composition and in vitro antioxidant and antimicrobial activities of the essential oils from Origanum syriacum L. growing in Turkey. *Biol Pharm Bull*. 26:1725-9.

5. Balgi, A.D., Fonseca, B.D., Donohue, E., Tsang, T.C.F., Lajoie, P., Proud, C.G., Nabi, I.R., Roberge, M. 2009. Screen for chemical modulators of autophagy reveals novel therapeutic inhibitors of mTORC1 signaling. *PLoS One* 4: e7124.

6. Ben Arfa, A., Combes, S., Preziosi-Belloy, L., Gontard, N., Chalier, P. 2006. Antimicrobial activity of carvacrol related to its chemical structure. *Lett Appl Microbiol.* 43:149-54.

7. Bi, X., Guo, N., Jin, J., Liu, J., Feng, H., Shi, J., Xiang, H., Wu, X., Dong, J., Hu, H., Yan, S., Yu, C., Wang, X., Deng, X., Yu, L. 2010. The global gene expression profile of

the model fungus Saccharomyces cerevisiae induced by thymol. *J Appl Microbiol.* 108:712-22.

8. Brett, C.L., Tukaye, D.N., Mukherjee, S., Rao, R. 2005. The yeast endosomal Na^+K^+/H^+ exchanger Nhx1 regulates cellular pH to control vesicle trafficking. *Mol Biol Cell*. 16:1396-405.

9. Dalleau, S., Cateau, E., Bergès, T., Berjeaud, J.M., Imbert, C. 2008. In vitro activity of terpenes against Candida biofilms. *Int J Antimicrob Agents.* 31:572-6.

10. De Martino, L., De Feo, V., Fratianni, F., Nazzaro, F. 2009. Chemistry, antioxidant, antibacterial and antifungal activities of volatile oils and their components. *Nat Prod Commun.* 4:1741-50.

11. DeRisi, J. L., Iyer, V. R., and Brown, P. O. 1997. Exploring the metabolic and genetic control of gene expression on a genomic scale. *Science* 278*:* 680-686

12. Forster, C. and Kane, P.M. 2000. Cytosolic Ca^{2+} homeostasis is a constitutive function of the V-ATPase in Saccharomyces cerevisiae. *J. Biol. Chem*. 275:38245-38253.

13. Gamarra, S., Rocha, E.M., Zhang, Y.Q., Park, S., Rao, R., Perlin, D.S. 2010. Mechanism of the synergistic effect of amiodarone and fluconazole in Candida albicans. *Antimicrob Agents Chemother*. 54:1753-61.

14. Gasch, A. P., Spellman, P. T., Kao, C. M., Carmel-Harel, O., Eisen, M. B., Storz, G., Botstein, D., and Brown, P. O. 2000. Genomic expression programs in the response of yeast cells to environmental changes. *Mol. Biol. Cell* 11: 4241-4257.

15. Gupta, S.S., Ton, V.K., Beaudry, V., Rulli, S., Cunningham, K., Rao, R. 2000. Antifungal activity of amiodarone is mediated by disruption of calcium homeostasis. *J Biol Chem.* 278:28831-9.

16. Hardwick, J. S., Kuruvilla, F. G., Tong, J. K., Shamji, A. F., and Schreiber, S. L. 1999. Rapamycin modulated transcription defines the subset of nutrient sensitive signaling pathways directly controlled by the TOR proteins. *Proc. Natl. Acad. Sci. U. S. A.* 96:14866-14870.

17. Martínez-Muñoz, G.A., Kane, P. 2008. Vacuolar and plasma membrane proton pumps collaborate to achieve cytosolic pH homeostasis in yeast. *J. Biol Chem.* 283:20309-19.

18. Mastelić, J., Jerković, I., Blazević, I., Poljak-Blazi, M., Borović, S., Ivancić-Baće, I., Smrecki, V., Zarković, N., Brcić-Kostic, K., Vikić-Topić, D., Müller, N. 2008. Comparative study on the antioxidant and biological activities of carvacrol, thymol, and eugenol derivatives. *J Agric Food Chem*. 56:3989-96.

19. Millard, P.I., Roth, B.L., Thi, H.P., Yue, S.T., Haugland, P.R. 1997. Development of the FUN-1 family of fluorescent probes for vacuole labeling and viability testing of yeasts. *Appl Environ Microbiol*. 63:2897-905.

20. Muend S, Rao R. 2008. Fungicidal activity of amiodarone is tightly coupled to calcium influx. *FEMS Yeast Res*. 8:425-31.

21. Pinto, E., Vale-Silva, L., Cavaleiro, C., Salgueiro, L. 2009. Antifungal activity of the clove essential oil from Syzygium aromaticum on Candida, Aspergillus and dermatophyte species. *J Med Microbiol*. 58:1454-62.

22. Pozzatti, P., Scheid, L.A., Spader, T.B., Atayde, M.L., Santurio, J.M., Alves, S.H. 2008. In vitro activity of essential oils extracted from plants used as spices against fluconazole-resistant and fluconazole-susceptible Candida spp. *Can J Microbiol*. 54:950-6.

23. Russo, M., Galletti, G.C., Bocchini, P. and Carnacini, A. 1998. Essential Oil Chemical Composition of Wild Populations of Italian Oregano Spice (*Origanum vulgare* ssp. *hirtum* (Link) Ietswaart): A Preliminary Evaluation of Their Use in Chemotaxonomy by Cluster Analysis. 1. Inflorescences *J. Agric. Food Chem.* 46: 3741–3746.

24. Salgueiro, L.R., Cavaleiro, C., Pinto, E., Pina-Vaz, C., Rodrigues, A.G., Palmeira, A., Tavares, C., Costa-de-Oliveira, S., Gonçalves, M.J., Martinez-de-Oliveira, J. 2003. Chemical composition and antifungal activity of the essential oil of Origanum virens on Candida species. *Planta Med*. 69:871-4.

25. Sherman, F. 1991. Getting started with yeast. *Methods Enzymol*. 194: p. 3-21.

26. Slamenova, D., Horvathova, E., Marsalkova, L., Wsolova, L. 2008. Carvacrol given to rats in drinking water reduces the level of DNA lesions induced in freshly isolated hepatocytes and testicular cells by H_2O_2. *Neoplasma.* 55:394-9.

27. Tampieri MP, Galuppi R, Macchioni F, Carelle MS, Falcioni L, Cioni PL, Morelli I. 2005. The inhibition of Candida albicans by selected essential oils and their major components. *Mycopathologia.* 159:339-45.

28. Ultee, A., Bennik, M.H., Moezelaar, R. 2002. The phenolic hydroxyl group of carvacrol is essential for action against the food-borne pathogen Bacillus cereus. *Appl Environ Microbiol*. 68:1561-8.

29. Warner, J.R. 1999. The economics of ribosome biosynthesis in yeast. *Trends Biochem Sci*. 24:437-40.

30. Xu J, Zhou F, Ji BP, Pei RS, Xu N. 2008. The antibacterial mechanism of carvacrol and thymol against Escherichia coli. *Lett Appl Microbiol*. 47:174-9.

31. Yoshimoto, H., Saltsman, K., Gasch, A. P., Li, H. X., Ogawa, N., Botstein, D., Brown, P. O., and Cyert, M. S. (2002*)* Genome-wide Analysis of Gene Expression Regulated by the Calcineurin/Crz1p Signaling Pathway in Saccharomyces cerevisiae. *J. Biol. Chem*. 277*,* 31079-31088

32. Zhang, Y.Q., Rao, R. 2007. Global disruption of cell cycle progression and nutrient response by the antifungal agent amiodarone. *J Biol Chem*. 282:37844-53.

33. Zhang, Y.Q., Gamarra, S., Garcia-Effron, G., Park, S., Perlin, D.S., Rao, R. 2010. Requirement for ergosterol in V-ATPase function underlies antifungal activity of azole drugs. *PLoS Pathog*. 6:e1000939.

Table 1. *Summary of differentially regulated genes in response to carvacrol*. Columns show numbers of genes that were altered by at least 2 fold.

Differential genes ≥2 fold	Carvacrol 0.005%	Carvacrol 0.01%	≥2 fold ratio (0.01% vs. 0.005%)
Up regulated	492	800	91
Down regulated	430	603	7

Table 2. *Representative examples of genes differentially regulated in response to carvacrol (0.01%)*. Only genes with altered transcription of at least 2-fold are shown. Categories shown have *P* values of <0.0005.

UP REGULATED	
Drug/ABC Transporters	SNQ2, PDR15, YOR1, VMR1, PDR11, PXA2, STE6, PDR18, PDR5, PDR10, PXA1
Autophagy	ATG1, ATG2, ATG3, ATG4, ATG5, ATG7, ATG8, ATG9, ATG14, ATG15, ATG16, ATG20, ATG22, PBN1, COX20, SNX4, LAP4, YPS1, STE13
Heat shock proteins & Chaperones	SSA1, SSA3, SSA4, HSP26, HSP42, HSP78, HSP82, HSP104, SSE2, MSS2, ECM10, MDJ1, FMO1, MPD1
Oxidative stress response	FRT2, PRX1, UGA2, GRX1, SNQ2, CTA1, TSA2, CTT1, GTT1, GPX1, SRX1, MCR1, FMP46, GAD1, GRE2, OXR1, GRE1
Energy reserve metabolism	TPS1, TPS2, GLC3, GSY1, GSY2, GSC2, PGM2
DOWN REGULATED	
rRNA processing	RPF2, UTP11, UTP13, UTP20, UTP23, RRP8, TSR1, TSR2, NOP4, ESF1, RRP1, RRP12
Ribosome biogenesis	RRP7, DBP6, RLI1, RSA4, RRB1, KRI1, NOP1, NOP7, NOP15, MAK16, MAK21
tRNA synthesis, processing	RPB5, LHP1, RPC52, BCD1, RPC10, RPC17, RET1, RPO40, RPO26, SEN34, POP8, POP6, SRM1
Pyrimidine metabolism	URA7, FUI1, FUR4, PRS3, DCD1, PPR1, URK1

Figure Legends

Figure 1. *Antifungal activity of Oregano oil and component terpenoid phenols*. *A*. Filter disks were soaked in serial dilutions of oregano oil and placed on a lawn of *S. cerevisiae*. Clear areas or halos were observed up to dilution of 1:8 and revealed inhibition of yeast growth. Controls show growth in the absence of essential oil. *B*. FUN-1 fluorescence (green) following treatment of yeast with oregano oil (described in Methods), but not with mineral oil, indicates loss of metabolic activity. *C*. Dose dependent effects on yeast growth of a panel of terpenoid phenols reveals structure-activity relationship. Inhibition of yeast growth followed the order carvacrol ≥ thymol > eugenol >> γ-terpinene, vanillin and guaicol. *D*. Time course of growth inhibition in the presence of 0.005%, 0.0075% and 0.01% of carvacrol. *E*. Dose dependent loss of metabolic activity in response to carvacrol was monitored using FUN-1 green fluorescence. Data represent average of triplicates.

Figure 2. *Disruption of ion homeostasis correlates with antifungal activity of carvacrol and terpenoid phenols*. *A*. Cytosolic Ca^{2+} was monitored by aequorin-coelenterazine luminescence as described in Methods. Addition of carvacrol (*arrow*) at the indicated doses elicited an immediate rise in cytosolic Ca^{2+} followed by rapid decay to baseline. Control response is in the presence of equivalent volume of solvent (ethanol). *B*. Ca^{2+}-induced luminescence in the panel of terpenoid phenols (0.05%; added at 20 s), varied in size and was proportional to their ability to inhibit yeast growth. *C*. Hypersensitivity to carvacrol in v*ma2Δ* null mutant, lacking V-ATPase activity, relative to isogenic wild type. Growth was monitored by Absorbance at 600 nm in synthetic defined medium as described in Methods. Measurement of vacuolar pH (*D*) or cytosolic pH (*E*) in response

to indicated concentrations of carvacrol, using compartment-specific pH sensitive fluorescent probes as described under Methods. Data are averages of triplicates.

Figure 3. *Functional distribution of genes differentially regulated by carvacrol.* Genes that showed transcriptional alteration by ≥2 fold in response to 0.01% carvacrol were categorized according to the MIPS classification system (see Methods). The inner circle shows functional categorization of the entire yeast genome, whereas the outer ring includes categories that were significantly over-represented in the carvacrol data set (*P* values $\leq 5 \times 10^{-3}$). Major functional categories represented in the carvacrol data set are listed on right. *A*. Up-regulated genes, *B*. Down-regulated genes.

Figure 4. *Carvacrol elicits transcriptional response similar to calcium stress and rapamycin.* (A) Hierarchical clustering of transcriptional response to carvacrol (15 min), $CaCl_2$ (5 & 30 min), rapamycin (30 min), thymol (90 min), time course series for diauxic shift, amiodarone, nitrogen depletion, and growth in YPD as described under Methods. Data available for 5468 genes were included in clustering analysis. Fold change values under each condition were $\log_2$ transformed and clustered with Gene Cluster 3.0. Distances between genes and arrays were computed based on correlation (centered). Both genes and arrays were clustered with average linkage method. The data were visualized with Java Tree View. Venn diagrams show the extent of overlap in the transcriptional response to carvacrol (0.005%, 15 min), calcium stress (30 min) and rapamycin (30 min) for up-regulated (B) and down-regulated genes (C).

1 **Figure 1.**

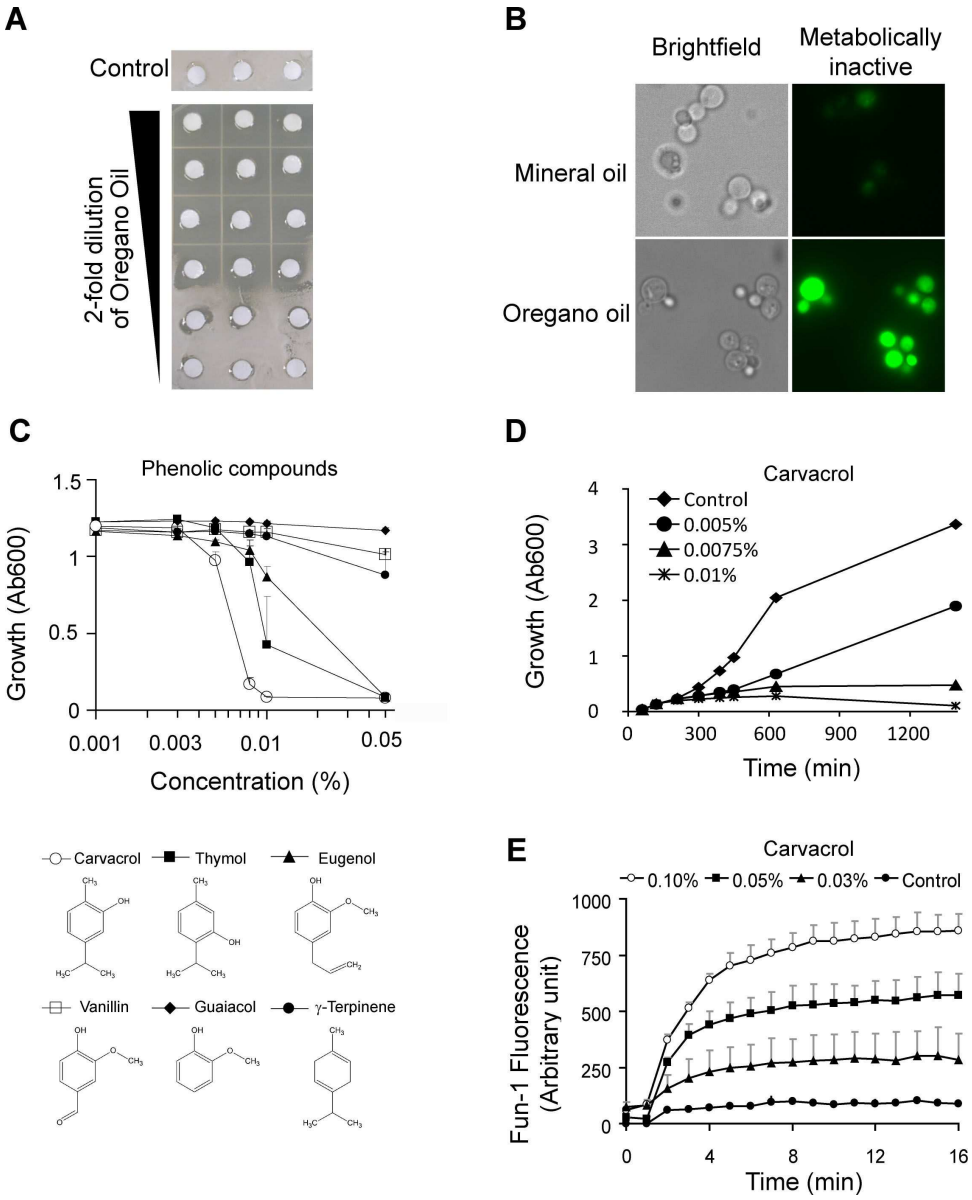

2

Figure 2.

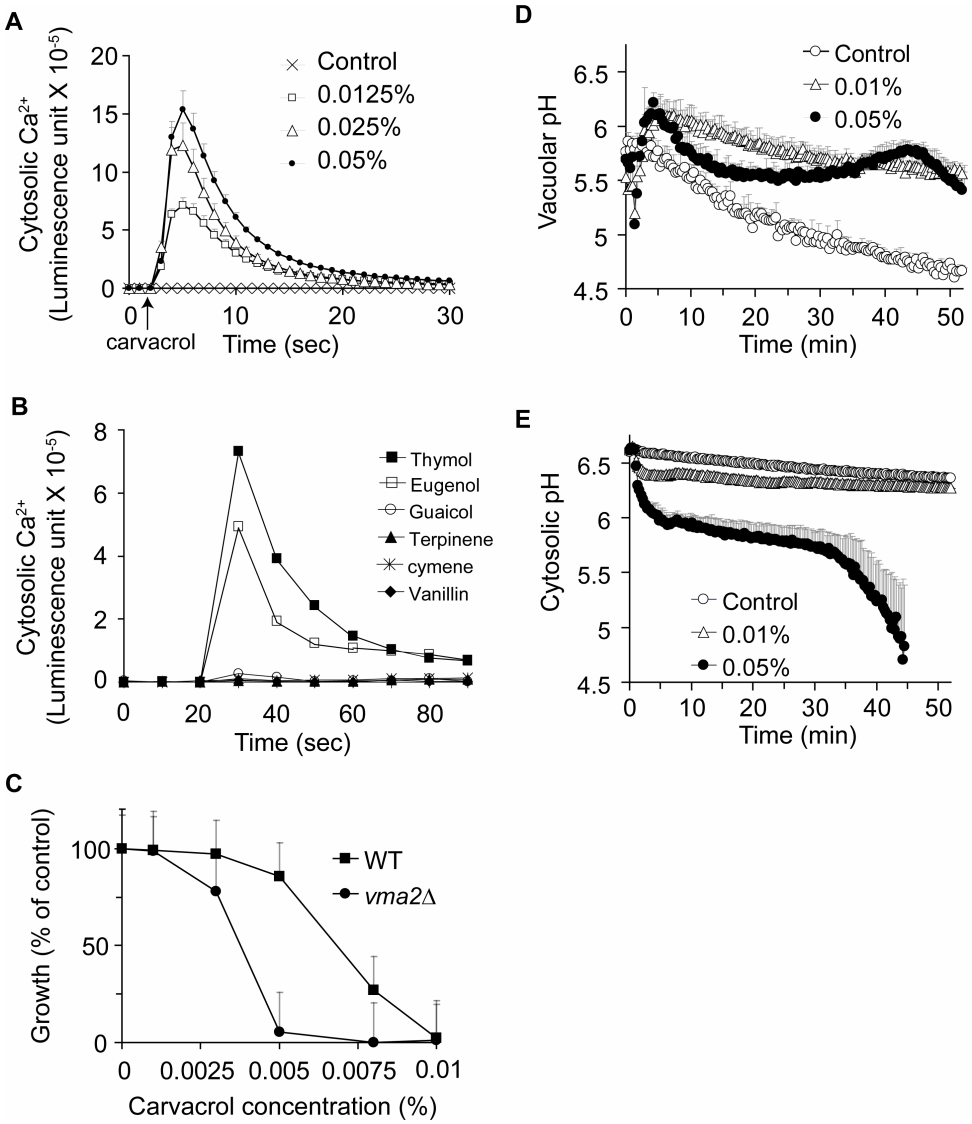

Figure 3.

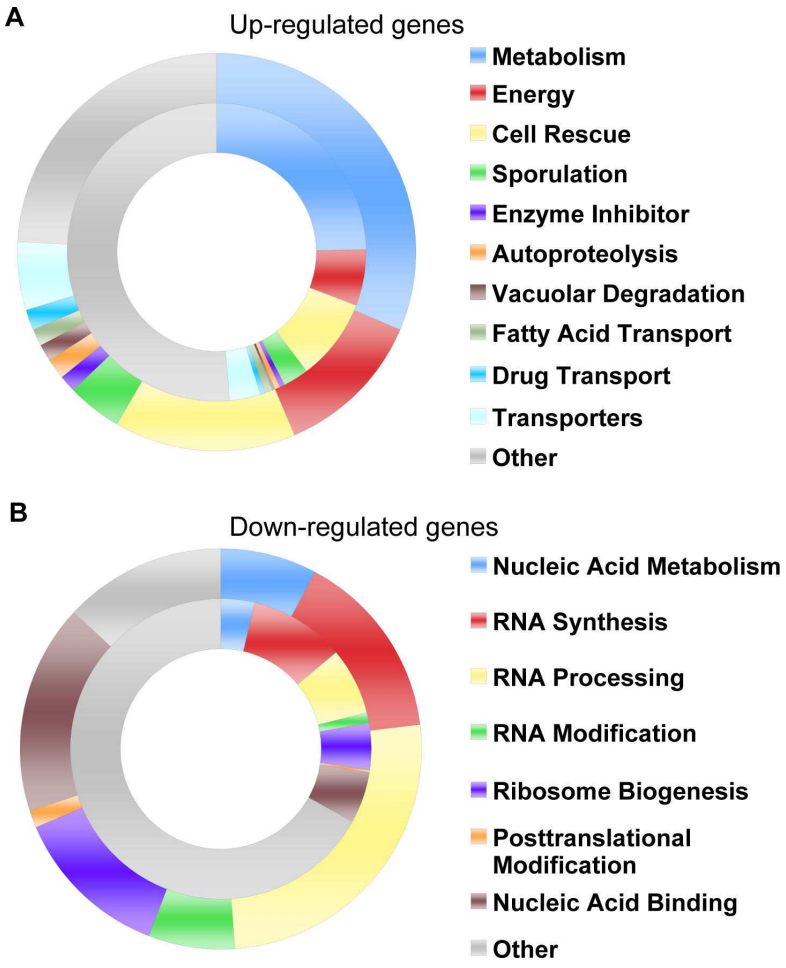

Figure 4.